SWOT platform contribution to overall Precise Orbit Determination

Carole Dufour[(1)], Fabien d'Este[(1)], Nathalie Steunou[(2)], Magali Tello[(2)]

[(1)] *Thales Alenia Space, 5 allée des Gabians, 06150 Cannes, France, +33492927000, carole.dufour@thalesaleniaspace.com ; fabien.deste@thalesaleniaspace.com*

[(2)]*Centre National des Etudes Spatiales, 18 avenue Edouard Belin, 31 Toulouse, France, +33561273131, nathalie.stenou@cnes.fr ; magali.tello@cnes.fr*

ABSTRACT

The CNES/NASA SWOT satellite (Surface Water and Ocean Topography) was launched on December 2022, and after successful commissioning and Calibration / Validation Phase, it began the first global survey of Earth's surface water and measurements of the circulation patterns of oceans. Preliminary science data shows excellent results, opening new perspectives in hydrology and oceanography fields.
Precise Orbit Determination is a prerequisite for altimetry measurements calibration, interpretation, and injection within any scientific work. Satellite characteristics reconstructions on ground have significant impact on the overall Precise Orbit Determination performances, both on frozen and varying shares. This paper addresses the SWOT platform contributions to the overall Precise Orbit Determination budgets. It will introduce the context and describe SWOT satellite focusing on key aspects regarding Precise Orbit Determination performances. Then it will review all the individual contributors at platform level, and provide insight in the specific analysis done at satellite level to assess whether associated uncertainty can be absorbed in the error budget or shall be corrected by dedicated model.

1 INTRODUCTION

The objective of this paper is to describe and quantify the SWOT satellite impact on the mission Precise Orbit Determination (POD)
In the first part, the paper recalls the mission context and the importance of the POD for altimetry measurement, in the second part the contributors to POD performances. Then, it focuses on the SWOT satellite contributions individually, and presents analytical approaches set in place to quantify and predict their impacts. Finally, it provides a satellite level performance estimation. The last part of the paper is dedicated to preliminary flight feed-back.

2 SWOT OVERVIEW

2.1 SWOT mission

SWOT satellite (Surface Water and Ocean Topography) is born from a cooperation between CNES and NASA. It was launched on December 2022, and after successful commissioning and Calibration / Validation Phase, it began the first global survey of Earth's surface water and measurements of the circulation patterns of oceans. Thanks to its wide-swath Ka-band radar interferometer, KaRIn (Ka band Radar Interferometer), combined with a nadir altimeter as well as support instruments, it offers a new opportunity for measuring the height of lakes, rivers and flood zones. It also enables cartography of mesoscale and sub-mesoscale circulation patterns on the oceans.

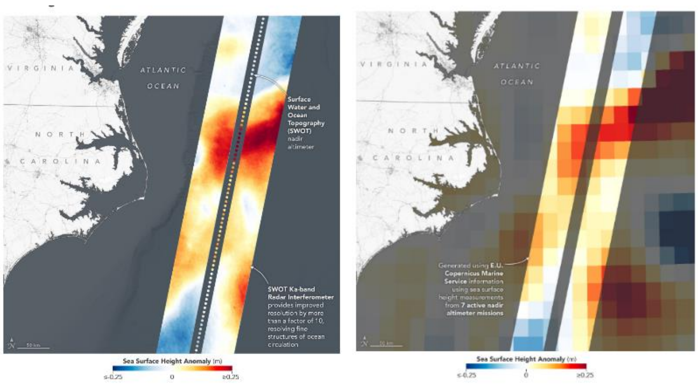

Figure 1. In the left, sea level data gathered on January 2023 by SWOT, which has 10 times the spatial resolution of the available data over the same area taken by altimeters on seven other satellites (right). Credit: NASA, swot.jpl.nasa.gov

SWOT satellite flies on a drifting low earth orbit (altitude near 900 km, inclination of 78 degrees) with a local nadir and track compensation guidance. This orbit enables a global coverage of the Earth surface every 21 days. Before reaching the operational orbit, the payload calibration has been performed on a 1-day repeat orbit a few kilometres below the current science orbit.
To comply with French and international regulations about space debris, SWOT satellite will be de-orbited at the end of its life in the Pacific Ocean with the first European controlled re-entry development.

2.2 SWOT Satellite

SWOT Satellite is divided into a platform developed by Thales Alenia Space and a payload module under Jet Propulsion Laboratory responsibility, integrating French and US instruments, as well as X-band telecom sub-system.

KaRIn instrument is a wide-swath Ka-band radar interferometer constituted of two reflectors perched at the end of two 5-meter masts. It is complemented by the Nadir altimeter, an Advanced Microwave Radiometer to correct altimetry data from atmospheric humidity, Doppler Orbitography and Radiopositioning Integrated by Satellite (DORIS) and Payload Global Positioning System (GPSP) for precise orbit measurements, and a Laser Reflect Array for independent position measurement from ground. All instruments and their antennas are integrated within a payload module (ref to figure 2) providing mechanical integrity, stability and thermal management.

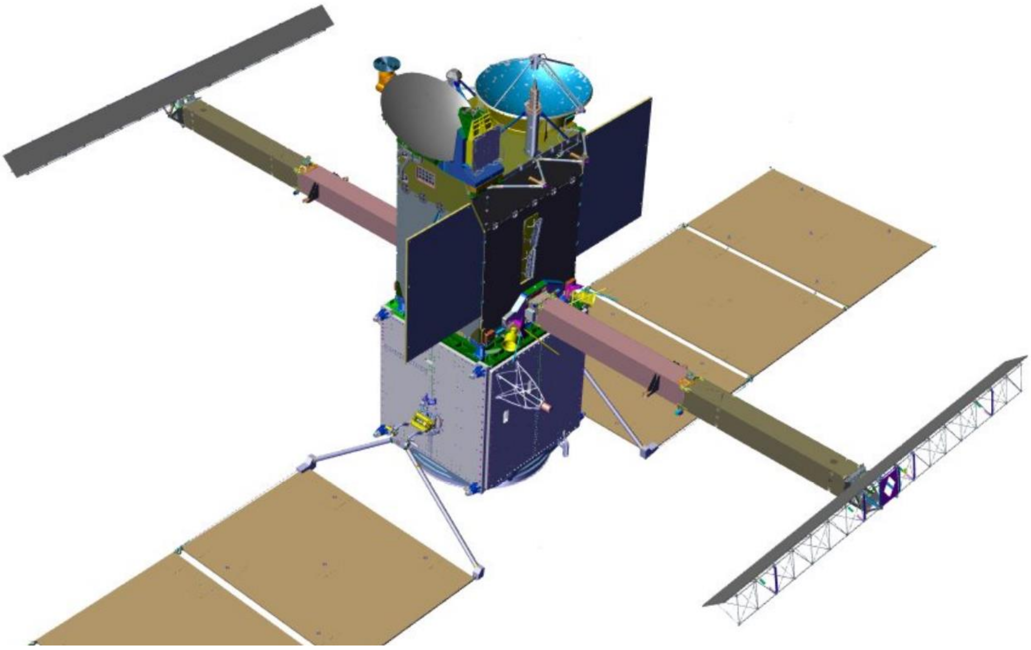

Figure 2. Payload module on the top of SWOT satellite

The platform (Ref to figure 3) provides all required services for satellite to survive the space environment and meet the mission needs in terms of attitude control, payload module pointing/stability and associated performances. An integrated avionics built around a core computer is in charge to manage all those services relying among others, on position and attitude sensors/actuators. It interfaces with ground to provide command and control capabilities, as well as science data storage and retrieval (mass memory). It is also responsible for providing orbit maintenance propulsive capabilities. To meet this objective, it accommodates a large tank with > 350 kg of propellant at launch, sized to actively de-orbit the satellite in the Pacific Ocean end of life. It transforms, stores and distributes power to the demanding payload. For that purpose, it features 36 m² solar panels attached through a bent yoke to solar arrays drive mechanism (SADM). This 3 pieces assembly allows maximizing the charge of a large battery as well as reducing shadowing effects to a minimum in order to cope with inclined, drifting orbit.

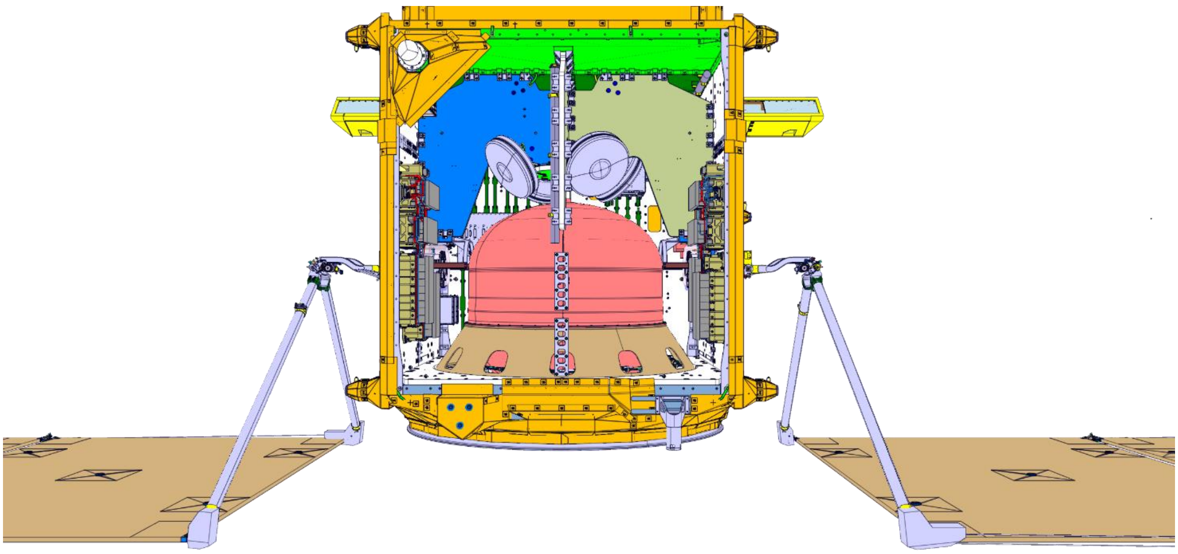

Figure 3 : Platform highlight on Tank and SA with bent yoke

2.3 Importance of POD for altimetry satellite

Satellite raw altimetry measurement provides the distance between the water surface and the instrument center of phase. In order to retrieve the water level, it shall be combined with orbital information, as well as fine localization of antennas with respect to the satellite center of gravity to reach the targeted sub-centimetric orbital accuracy (radial direction). Improvement in the modeling of Earth's gravity field and ocean tides, coupled with progresses made in the observation methods used for altimetry satellites (DORIS & GPSP specifically for SWOT) allows to reach these performance objectives.

The fundamental vector provided by POD is from the Center of Mass of the Earth system to the center of mass of the satellite. An orbit height error directly translates into a height error of the same amount, both on KaRIn and Nadir altimeter products, since the desired topographic measurement assumes perfect knowledge of the orbit's altitude. As a consequence, POD errors shall be limited to a minimum and have been subjected a to dedicated works in the specification & development phases.

2.4 POD performances apportionment for SWOT mission

On SWOT satellite, the POD requirements are identical as the ones applicable to the Jason series (typically 1.5cm rms @ 1-sigma for ocean and wavelengths above 1000km and hydrology needs), despite a factor 2 on the satellite body dimensions, a factor 4 on solar arrays surface and overall satellite mass, and a factor > 10 on the propellant mass. This sharpens the challenges on the satellite hardware contributions to the POD performances, and justifies the need for specific approaches.

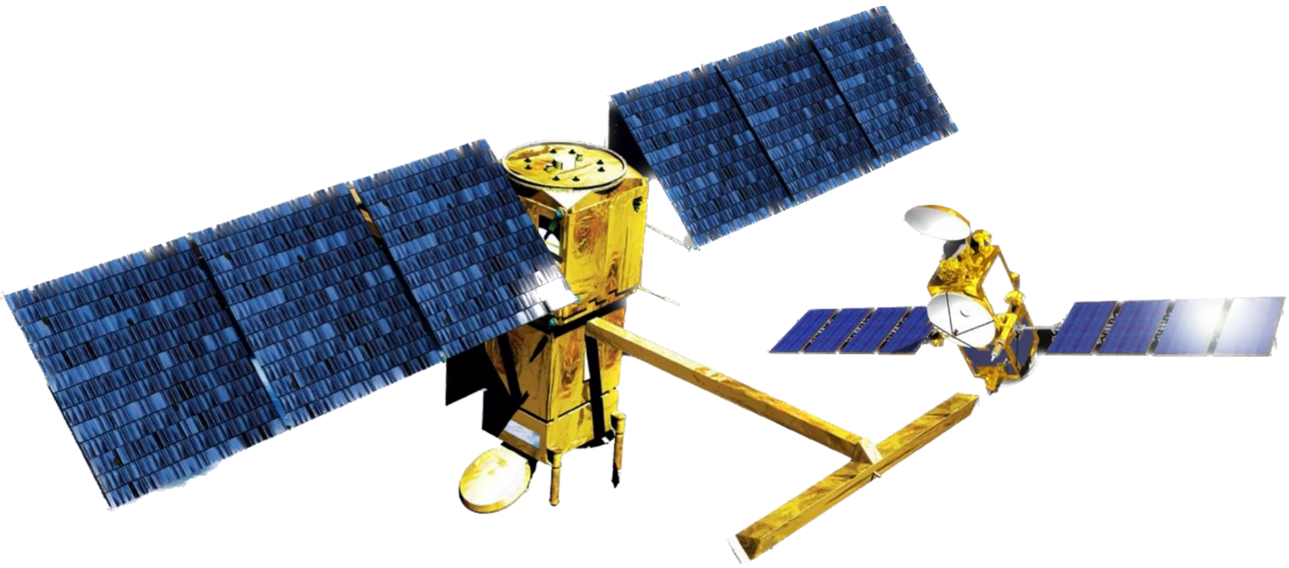

Figure 4 : SWOT and Jason 3 size comparison

POD performances includes POD instruments performances (Doris, GPSP, LRA) and the ground reconstruction, with modeling errors of atmospheric drag, solar radiation pressure, gravitational effects and model of the S/C. It also includes knowledge of the antenna phase center position for the different instruments.

Another contributor is the knowledge of the Flight System center of mass. This is fully allocated to the satellite, with some payload center of mass inputs. As Jason-like constraint on maximum center of mass position knowledge error of 5mm per axis merging all possible effects was out of reach, the total tolerated error has been relaxed, but specific constraints have been added on three different frequency ranges:

- Static knowledge errors refer to errors at the beginning of on-orbit operations, so it contains all the uncertainties before that state (measurements uncertainties, modelling errors, 0g, deployment of

KaRIn antennas); these components can be partly adjusted during checkout phase, at the beginning of processing.
- Orbital variations refer to all the unknown variations along the orbit (typically thermoelastic effects).
- Long term variations refer to all the unknown variations occurring with a period higher than 10 days (propellant consumption due to orbit control, thermoelastic induced by beta angle). Part of it is predictable, for instance propellant consumption impact on satellite center of mass position is estimated.

This specification method (see [1] for more details) allowed to limit as much as possible the amount of variations over an orbit duration, as they cause the most damageable errors: indeed, they cannot be distinguished from a noise and thus degrade the error budget.

Although this dedicated apportionment method has created a "requirement space" favorable for SWOT satellite to meet the challenging POD needs of the science mission, the expected level of error can be reached only with accurate geometrical characterization of the satellite, as well as modeling of many mission-dependent parameters with the highest representativeness. Methodology to minimize all satellite dependent error sources will be described in this article.

3 CONTRIBUTIONS OF FLIGHT SEGMENT IN POD PERFORMANCES

Among the POD performance contributors discussed above, some are in the hand of the instrument or ground teams. But many satellite parameters play a role in the flight segment contribution to POD reconstruction. Each of them needs to be characterized as accurately as possible in order to reconstruct with precision the positioning of antennas center of phases and bore sight axis relative to satellite center of mass.

The following types of contributions are addressed at satellite level :
- Antennas boresight and center of phase positioning on ground
- Antennas boresight and center of phase displacement in flight
- Satellite CoG position knowledge

This section defines each contribution and describes how it is measured or predicted to best fit the actual satellite geometry.
In order to work in a well-defined and materialized reference frame, all on-board position vectors are discussed and expressed with respect to the satellite mechanical reference frame.

3.1 Antennas boresight and center of phase positioning on ground

On-ground, satellite geometry can be measured through dedicated metrology campaign. When relevant for science data accuracy, the antennas center of phase location (respectively boresight alignment) is materialized through a set of visual targets or pin balls (respectively corner cubes). This enables the measurement of these critical characteristics after units assembly in a higher level module, and fine characterization of position and orientation in the satellite reference frame.
These operations are run several times along the Assembly, Integration and Test (AIT) campaign via the photogrammetry technique, providing the most accurate reference and monitoring any unexpected motion during the AIT process. Metrology campaigns also anticipated on the KaRIn deployment ant provided alignment and positioning data to extrapolate on the deployed system.

Note that when positioning knowledge is not critical in the overall performance, antennas are not necessarily equipped with metrology device and can be positioned via structural design and manufacturing only. In this case, slacks in links or inaccuracy in drilling realization are not measured and directly translates into positioning errors. On SWOT satellite this is the case for GPSP antenna, which can be positioned with accuracy better than 1mm in satellite reference frame, only relying on the structural manufacturing and assembly precision.

3.2 Antennas boresight and center of phase displacement in flight

All flight effects impacting the relative positioning and alignment of antennas and satellite reference frame are linked to thermo-elastic distortion. Indeed, no other mechanical or degree of freedom within the satellite body impact the antenna positions after deployment. To quantify these distortions, and assess whether it is required to predict them, HW thermal maps analyzed on worst orbital cases, and fed to a Finite Element Model. On SWOT, satellite body is a stiff aluminum box, limiting gradients and thus thermoelastic distortions.
Large appendices, such as the solar arrays, display much more significant displacements, but only impact the orbit determination performances through the center of mass displacement (see 4.3), and do not generate antennas displacement in flight.
Finally, KaRIn masts are also very sensitive due to their large dimensions, but their critical stability needs have been accounted for early in the design phases, resulting in stiff and inert behavior with no significant thermos-mechanical impact on the feeds / reflector system distortion.
Resulting displacements are within expected tolerances, justifying the absence of need of predicting models.

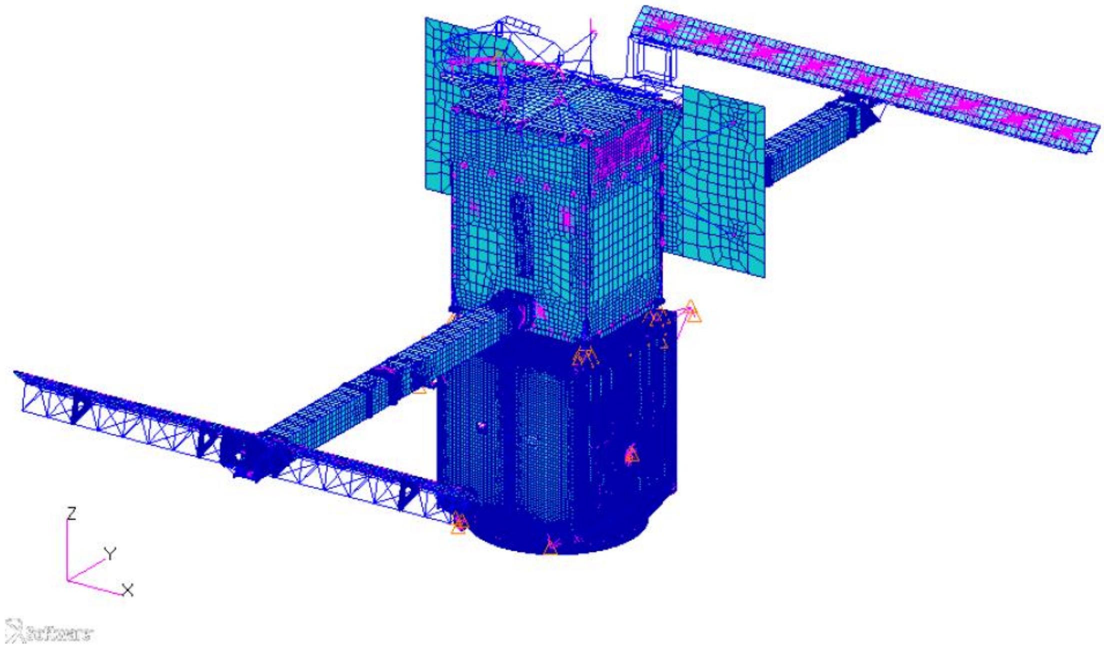

Figure 5 : View of SWOT Satellite FEM

3.3 Satellite CoG position

After having positioned precisely the antennas with respect to the satellite reference frame, another key aspect is to accurately reconstruct the location of the satellite center of gravity in the same reference. Indeed, all motion propagation equations rely on Earth gravity field, and apply to center of mass.

Prediction of Satellite CoG location is based on several individual activities :

- Mass properties measurement during the AIT sequence, where mass, center of mass and inertia are measured accurately in the current satellite configuration.
- Extrapolation to flight configuration is done by compensating for discrepancies between measured and flight configurations (deployed solar arrays, deployed payload, test hardware removal, tank filled with propellant…)
- Day to day flight events are then modelled and impact on center of mass is predicted
    - Flight telemetry provides current solar arrays orientations. Coupled with the characterization of the solar wing geometry and center of mass location performed on ground before launch, it allows to recompute the impact of the large appendices on the satellite center of mass

- Similarly, flight telemetry gives pressure and temperature information at the tank location. This enables computation of the remaining propellant mass, and its injection in the Satellite centering analysis.

Figure 5 : SWOT MCI test

§4 will provide more details on modeling approaches for satellite center of mass position reconstruction.

4 MAJOR CONTROBUTORS IMPACT REFINEMENTS AND MODELING APPROACH

This chapter focuses on three components of the satellite whose evolutions during flight impact the satellite center of mass. For each of them, the impact of its evolution during flight will be presented. Then, an approach allowing to model and predict the evolution will be discussed. The remaining uncertainty, as well as the variation timescales are evoked.

4.1 Propellant mass

4.1.1 Impact on satellite Center of mass position knowledge

In order to provide enough impulse for orbit acquisition, maintenance, and end of life disposal, SWOT satellite embarks 358 kg of propellant. Given the tank accommodation in the platform, satellite center of mass with full tank or at end of mission will change by more than 200 mm, which is 2 orders of magnitude above the tolerated knowledge uncertainty.
Even if the center of mass position knowledge accuracy is only requested for science needs, excluding the controlled re-entry propellant consumption from the scope of fine reconstitution, this still leaves with more than 35 mm center of mass motion due to this post. This has to be modeled and predicted to retrieve satisfactory orbit determination.

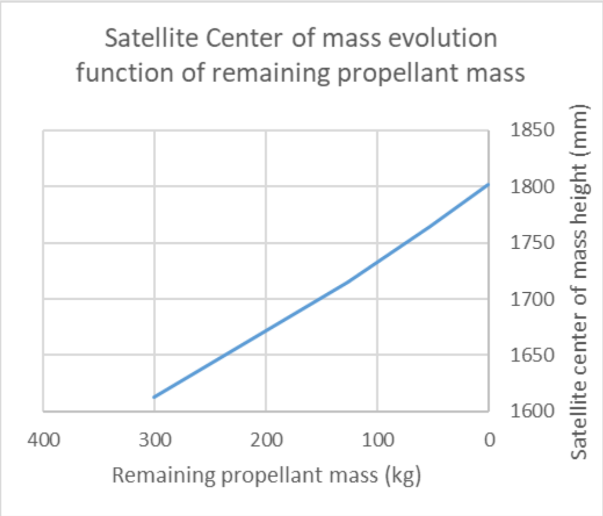

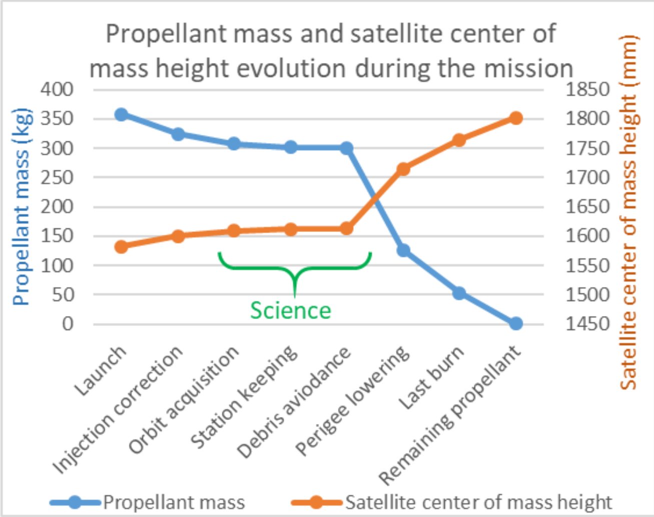

Figure 6 : Left : satellite center of mass function of remaining propellant mass.
Right : Propellant mass and satellite center of mass height evolution along the mission illustrates the need for modelling to retrieve accurate POD during the science mission

4.1.2 Modelling approach

SWOT propellant tank is a diaphragm tanks operated in blow-down mode. As such, the propellant part is filled with 358 kg of propellant right before launch, then the upper part is pressurized with gaseous nitrogen to up to 26 bars. The applied pressure expulses the propellant towards the thrusters when valves are open. As a consequence, the gas pressure measurement, coupled with a temperature sensor, enables an estimation of the remaining propellant mass via the Pressure Volume, Temperature method.

$$M_{propellant} = \rho_{propellant} \times \left(V_{Tank} - \frac{P_{N_2}^0 . V_{N_2}^0}{T_{N_2}^0} . \frac{T_{N_2}}{P_{N_2}} \right)$$

Where:

$M_{propellant}$ is the remaining propellant mass in the tank
$\rho_{propellant}$ is the volumic mass of the propellant
V_{Tank} is the tank total volume
$P_{N_2}^0$ is the initial nitrogen pressure
$V_{N_2}^0$ is the initial nitrogen volume
$T_{N_2}^0$ is the initial nitrogen temperature
T_{N_2} is the flight telemetry for nitrogen temperature in the tank gas shell
P_{N_2} is the flight telemetry for nitrogen pressure in the tank gas shell

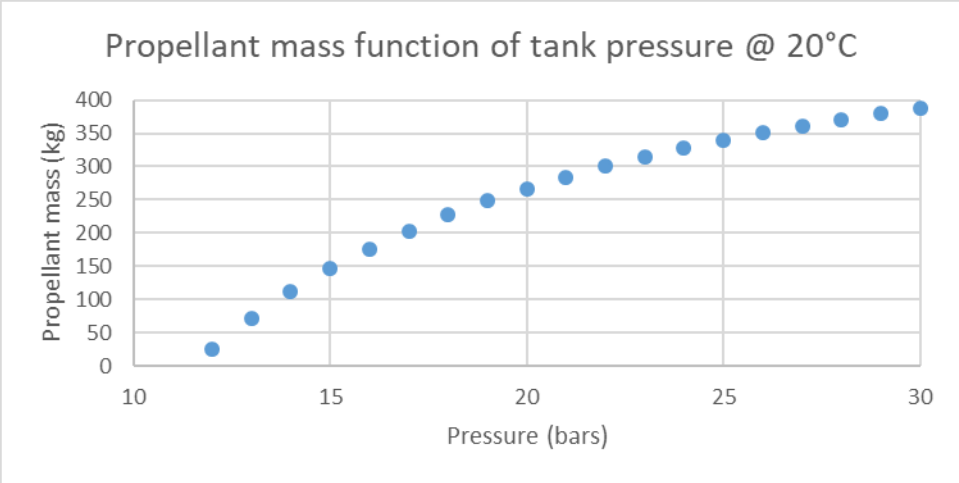

Figure 7 : Propellant mass function of flight nitrogen pressure measurement @ 20°C

4.1.3 Residual uncertainty

From the modelled equations, one can also derive the associated uncertainty depending on the flight telemetries and initial measures uncertainties :

$$dM_{propellant} = \rho_{propellant} \times n_{N_2}.R\left(\frac{dT_{N_2}}{P_{N_2}} + T_{N_2}\frac{dP_{N_2}}{{P_{N_2}}^2}\right)$$

In flight, propulsion module temperature remains very close to 20°C. For this temperature, graph Figure 8 shows the pressure evolution and associated propellant mass estimation uncertainty, modeled as a function of remaining propellant mass. Theoretical error maximum boundary is derived to 8 kg at end of science mission, which corresponds to 4 mm on the radial axis.

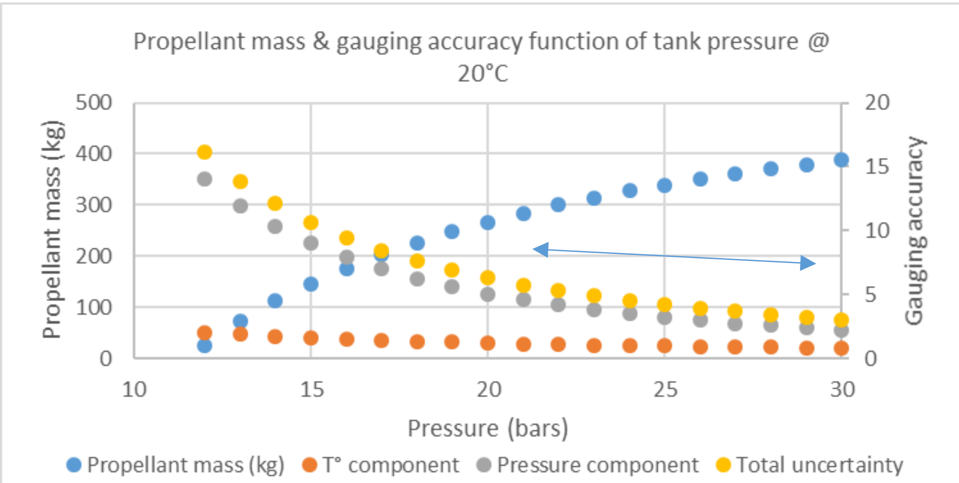

Figure 8 : Propellant mass and gauging accuracies identifying compoentnes due to T° measurment uncertainty and pressure measurement uncertainty. Performance is only requiredd for science mission.

However, a fair share of these 8 kg is an initial bias, which is calibrated to 3.9kg by confronting the gauging method results in flight before first thrusters boost to the very accurate ground measurement of the loaded propellant mass. After calibration, one can see in flight that the difference between the predicted versus measured propellant mass consumption is of the order of 50g, justifying the good stability of the mass determination model, and the accurate representativeness of the analytical predictions.

Overall, the maximum propellant mass error after calibration can be bounded to 4.1 kg, which corresponds to a radial error on satellite center of mass position of 2.1 mm.

4.1.4 Discussion on time scales

In flight, propellant mass only evolves when an orbit control manoeuver is realized. In order to maintain the satellite in the desired flight window, and now that the science orbit has been reached, it is estimated to perform one orbit control manoeuver about every 40 days. In addition, few debris avoidance manoeuvres are to be realized every year. This justifies the allocation of this post to the long term budget.

4.2 Propellant center of mass

4.2.1 Impact on satellite Center of mass position knowledge

The estimation of remaining propellant mass and the associated uncertainty has been addressed in previous section. In addition, consuming propellant in a blow-down tank drives down the remaining propellant center of mass. Over the range of propellant masses covered during the SWOT science mission, the propellant center of mass is estimated to move by ~80 mm, which impact the satellite center of mass by ~13mm. This is significant versus the requested performances, thus needs to be predicted.

4.2.2 Modelling approach

Propellant part of the tank is an ellipsoid, whose semi major and semi minor axis are given in the tank datasheet.

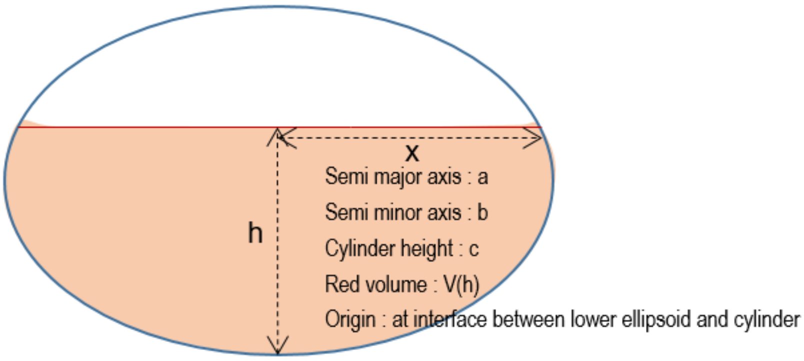

Figure 9 : Schematical representation of the propellant shell, with geometry justifying the analytical mass, volume and center of mass derivation.

From these geometrical information, and assuming a perfectly horizontal liquid surface, one can :

- Analytically compute the propellant mass and volume as functions of the propellant height

$$V(H) = \int_{z=-b}^{z=H} \pi . x^2(z)\, dz$$

- Analytically Compute the propellant center of mass height as a function of the propellant height

$$\overrightarrow{OG} = \frac{1}{m_{tot}} \int_{V(H)} \overrightarrow{OP}\ dm = \frac{1}{\rho . V(H)} \int_{-b}^{H} z . \pi . x^2(z) . \rho . dz$$

- Combine both numerical datasets to extract the propellant center of mass height as a function of the propellant mass
    - Comparison with tank provider (ATK) data points confirms the correct theoretical derivation

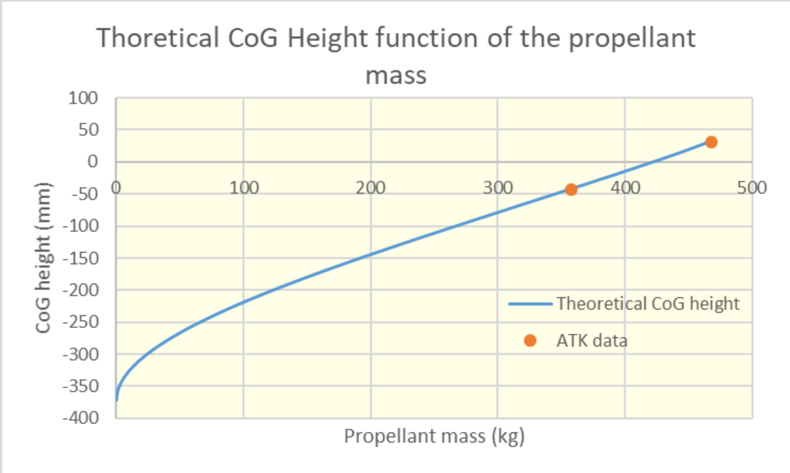

Figure 10 : Resulting analytical evolution of the propellant center of mass function of remaining mass in the tank. Comparison with tank supplier commited data confirms representativeness.

4.2.3 Residual uncertainty

Analytical approach presented above is used to correct the satellite center of mass position from the propellant center of mass motion during the mission. It assumes a perfectly horizontal propellant surface. However, the diaphragm has its own stiffness and its shape is driven by the need to match the tank lower shell in order to reduce residuals when tank is empty. Consequently, when tank is partially filled, the diaphragm shape is disturbed (see Figure 11), which leads to deviation of propellant center of mass position with respect to theoretical approach.

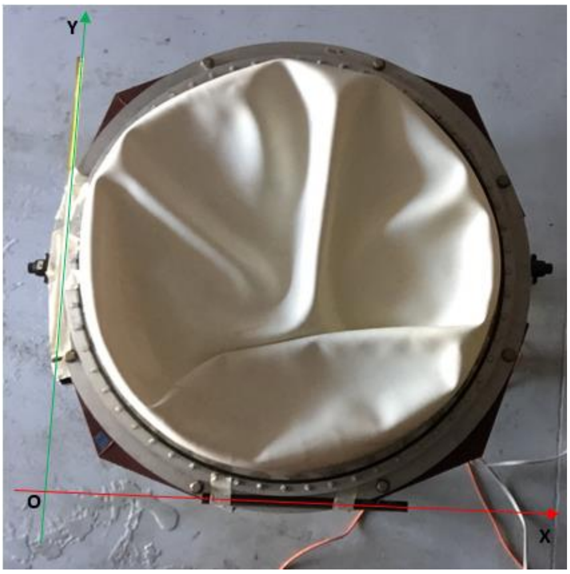

Figure 11 : SWOT tank diaphram. It illustrates stiffness and non-flat surface at partial filling ratio.

To quantify the residual errors, Thales Alenia Space requested a specific test to the tank provider (Orbital ATK). This test aimed at measuring the center of gravity migration in the ATK 40 inch diaphragm tank for different fill levels. The measures are performed for 20 fill and drain cycles, in order to evaluate the repeatability of the observed phenomenon, and derive statistics on the errors. The 3-D scanner provides a 3D map of the diaphragm surface, then the mass distribution of the propellant and its center of mass can be found.

Table below shows the 340L scan for 5 different data sets. This shows the overall same symmetry level, while some of them have marks deeper than others.

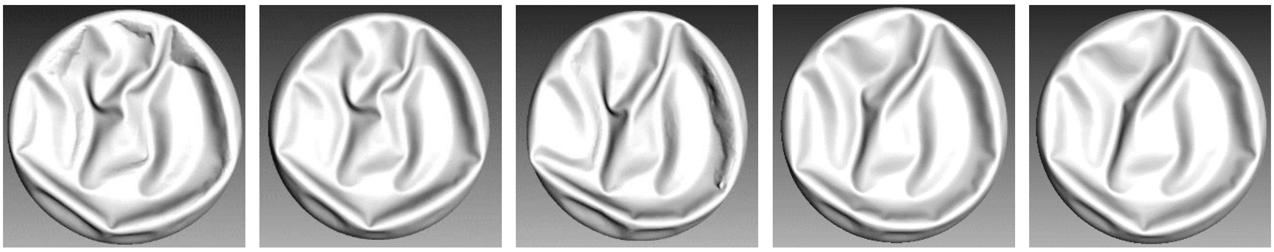

Figure 12: Diaphragm surface scans for same filling ration (340L) for 5 different repetitions from ATK SWOT dedicated tests.

The distribution of the in plane center of mass location is shown on figure 13, and enables to derive a 1 sigma and 3 sigma remaining error. Similar approach is applied for the out of plane deviation from the theoretical model. Combined with uncertainty sources listed in Orbital ATK test report, such as 3-D scanner accuracy, temperature error or propellant mass error, the overall uncertainty budget is given in Figure 14, and is reduced by a factor 10 with respect to the uncorrected out of plane value.

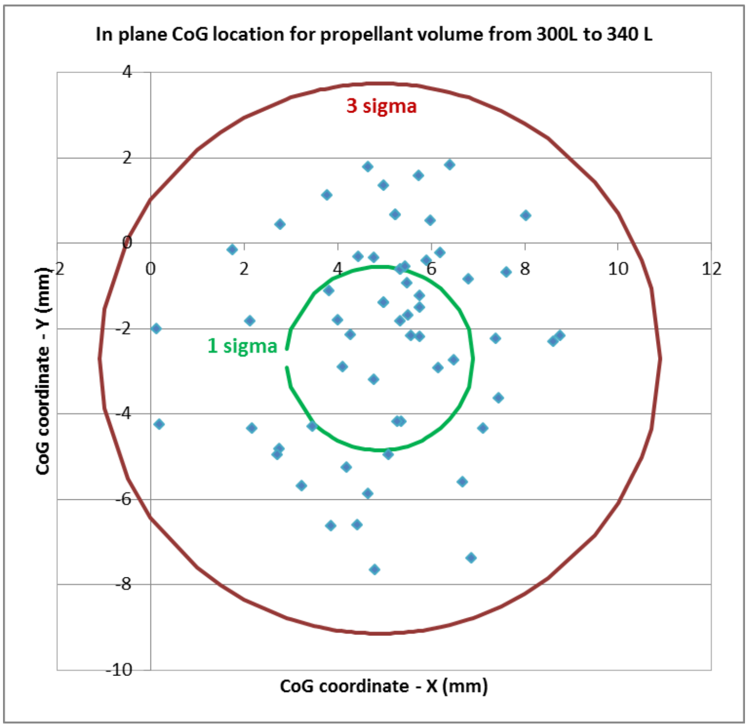

Figure 13: In-plane propellant center of mass location distribution for 20 repetitions, for filling ratio consistent with SWOT science mission ranges. 1sigma and 3 sigma unbalances can be defined.

Propellant CoG position knowledge	X [mm]	Y [mm]	Z [mm]
Ecart type	2.00	2.15	2.89
Dataset uncertainty	10.91	9.14	8.67
Fidelity (1)	1.44	1.62	2.19
Temperature variability (1)	0.3		
Resolution (1)	0.022		
Error on propellant volume	NA	NA	0.42
Uncertainty at propellant level	**11.01**	**9.29**	**8.95**
Uncertainty at satellite level	**1.87**	**1.58**	**1.52**

(1) From ATK center of mass migration test report

Figure 14 : Uncertainty budgets for in plane and out of plane propellant center of gravity position and impact at satellite center of mass location level (last line)

4.2.4 Discussion on time scales

Diaphragm will undergo high constraints during launch, but after that, the accelerations applied on the satellite are very limited.

The order of magnitude of the loads at play after launch has been evaluated and compared, in order to conclude on the diaphragm behavior during the mission and assess if the propellant center of mass position uncertainty shall be classified as a static error or a long term variation.

The following loads tend to induce a motion on the propellant :

- Nadir pointing maintenance
- Angular rotation due to attitude control
- Angular acceleration due to attitude control
- Thrust during Orbit Control Maneuvers

Other forces tend to prevent the motion of the propellant within the tank :

- Laplace pressure
- Diaphragm stiffness
- Delta pressure during maneuvers

Tables below provide additional information and order of magnitude evaluation for each force at play.

Motion inducing forces	Direction	Lever arm	Acceleration on propellant
Nadir pointing maintenance 1 rotation in 1 orbit (10-3 rad/s)	Radial	R orbit = 6378 + 890 km	1x10-6 m/s²
Max satellite angular rates (2.2°/s)	Radial	Prop. Cog to Sat CoG # 1m	1.5x10-6 m/s²
Max satellite angular accelerations (0.02 °/s²)	Tangential	Prop. Cog to Sat CoG # 1m	3.5x10-4 m/s²
Orbit control maneuver thrust (0.08 m/s²)	Along +Z	NA	0.08 m/s²

Motion opposed forces	Direction	Constraint	Acceleration on propellant
Laplace pressure	Axial	2.7 N/m²	0.05 m/s²
Diaphragm stiffness	Unknown – assumed negligible for conservatism		
Delta pressure during maneuvers	Unknown – assumed negligible for conservatism		

Figure 15 : Motion inducing and motion opposed forces inventory and quantitative assessment.

As shown in those tables, excepted for the orbit control thrust, all motion inducing forces amplitudes are negligible face to the Laplace pressure. This means that the attitude control of the spacecraft will not lead to propellant motion in the tank.

Regarding the Orbit Control Maneuver thrust, its impact on propellant is of the same order of magnitude as the Laplace pressure. As its direction is aligned to the +Z vector, all the loads impacting the propellant location in the tank are aligned to the same vector (gravity on ground, last launcher boost, thrust). Last launch loads being much more significant than the orbit control maneuvers, they will drive the diaphragm shape, and the propellant center of mass location.

After launch, no radial loads are big enough to counter the Laplace pressure, thus the diaphragm shape will remain the same until the end of the mission.

Consequently, that propellant center of mass error can be considered as a bias in the center of mass position knowledge budgets.

4.3 Solar arrays Center of mass

4.3.1 Impact on satellite Center of mass position knowledge

Solar Array wings Center of mass is not aligned with its rotation axis. As a consequence, the angular position of the wings has a strong impact on the satellite center of mass position, which needs to be modeled in order to avoid satellite center of mass position knowledge error of 30 mm.

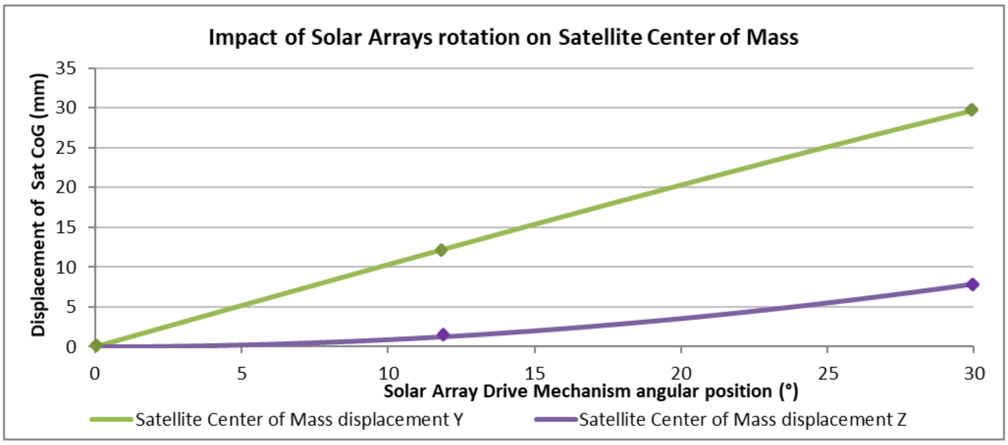

Figure 16 : when solar arrays orientation is shifted to follow season, the satellite center of mass is impacted significantly.

In addition to the basic geometrical rotation of a perfect wing around a perfectly oriented SADM axis, with a perfect initial “0°” position, the following effects are measured to refine the solar arrays center of mass position knowledge :

- The solar array mass and center of mass position after wing deployment to precisely represent the geometry of the rotating part
- The SADM position and orientation in satellite reference frame to precisely know the rotation axis
- The SADM axis orientation for the initial “0°” position (the canonical position) after deployment to precisely know the reference point.

4.3.2 Modelling approach

The model implemented to compute the solar arrays center of mass location consists in combining the translations and rotations leading from the solar array reference frame (figure 17), in which the wing center of mass is characterized, to the satellite reference frame, in which the satellite center of mass is computed. Rotations angles come from integration sequence measurement or flight telemetry, and translations are characterized by vectors measured during integration.

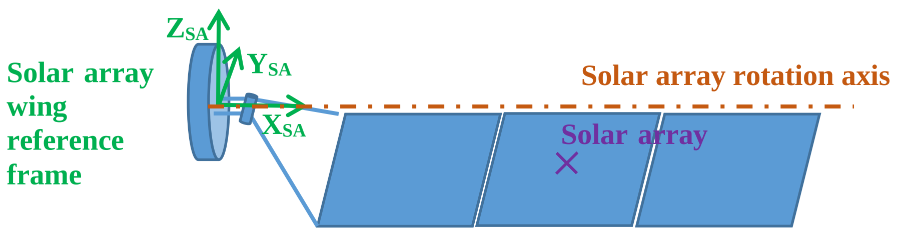

Figure 17 : Solar arrays wing center of mass, rotation axis, and reference frame.

Each transformation is described via its associated matrix. The final combination of all matrices gives the Wing CoG position in the satellite reference frame.

$$\left(\overrightarrow{O_{Obs}G_{wing}}\right)^{Obs} = \underbrace{\left(\overrightarrow{O_{Obs}O_{SA}}\right)^{Obs}}_{\text{SADM theoretical position}} + \underbrace{M_{OBS\to SADM\_0}}_{\text{SADM theoretical orientation}} \times \underbrace{M_{SADM\_0\to SA\_0}}_{\text{SADM reference angular error}} \times \underbrace{M_{SA\_0\to SA\_\theta}}_{\text{Solar array flight orientation}} \times \underbrace{\left(\overrightarrow{O_{SA}G_{wing}}\right)^{SA}}_{\text{Solar array center of mass in wing frame}}$$

Figure 18 : Matrices combination leading to define solar arrays center of mass location in satellite reference frame.

4.3.3 Residual uncertainty

All parameters used as constants in the model described above are measured during the solar array or satellite assembly to a certain accuracy. The remaining uncertainty translates into an satellite center of mass position estimation error.

Given the small amplitudes of all uncertainties, Taylor expansion allows to linearize the differential expression and evaluate independently all error sources.

- Solar array facility scale accuracy is 0.4% of the measured mass. This leads to uncertainty of 0.5 kg at wing level, translating to an error up to few tenth of mm on satellite center of mass position estimation on Y & Z axes depending on the solar arrays orientation
- Deployed Solar array wings center of mass position in micro-gravity also comes from a combination of measurement and prediction. Each wing geometry is measured with a gravity compensation set-up, then geometry is combined with element mass information to localize the center of mass. While wing deflection can lead to out of plane bias of up to 60mm, the reproducibility is quite good and, after calibration, residual error on this axis is reduced by a factor 10. Note that only out of plane deflection can be corrected via ground measurements. In plane errors cannot be compensated and can reach up to 20 mm, impacting satellite center of mass knowledge accuracy by up to 1.5mm.
- Solar array rotation axis has been measured in the integration flow. Its misalignment to the perfect +X direction is very low (0.03° on Y and 0.01° on Z), and thus is not corrected in the model. Equivalent impact on the satellite center of mass accuracy is < 0.1mm.
- Solar array angular position around its rotation axis also bears some uncertainties :
    - On the initial reference position, characterized in the integration flow to an accuracy of 0.08°

- On the flight orientation knowledge whose accuracy is also 0.08°
- Corresponding error on satellite center of mass reaches 0.2mm depending on the solar arrays orientation

All those effects impact the satellite center of mass, depending of the solar array orientation, but they are caused by independent phenomenon. As a consequence, they are summed quadratically to assess the overall error on satellite center of mass due to solar arrays sources to ~1.5mm per axis

	Unit level uncertainty	Error on satellite center of mass position [mm]
Solar wing mass	0.5 kg	0.2
Solar wing deployed configuration center of mass	20mm	1.5
Solar wing rotation axes	0.03°	0.1
Solar wing angular reference	0.16°	0.2
Equivalent total impact of solar arrays contributions		1.53

Figure 19: Total solar arrays contribution on the satellite center of mass position knowledge error

4.3.4 Discussion on time scales

Among solar arrays related errors, some are AIT measurement bias that will not change during the satellite life time after deployment (wing mass or center of mass location in wing frame), and other depends on the mission season (commanded solar arrays angular position)
However, the solar array wings center of mass is not aligned with the rotation axis, so when the solar array rotates, the error distribution along Y & Z axis changes. As a result, even if the error source is static in the reference frame linked to the SA wing, it is dynamic with long term evolutions in the satellite reference frame. Consequently, all solar arrays related errors are accounted for in the long term error budget, excepted for the thermos-elastic distortion which varies at orbital period.

5 ASSESSMENT OF ERROR SOURCES AT FLIGHT SEGMENT LEVEL

Four types of errors coming from the satellite hardware impact the relative position of antenna center of phase and satellite center of mass, and consequently the overall orbit determination performance :

- Ground measurement inaccuracy
- Flight measurement inaccuracy
- Model inaccuracy
- Non modelled error sources

As seen above, ground and flight measurements are input for [SN1]models [SN2] at predicting the remaining propellant mass, the propellant center of mass location, and the solar arrays center of mass with an accuracy inside the needed ranges for mission performance. Other sources of uncertainties are discussed in this chapter, and satellite level performances including all error sources are presented.

5.1 Antennas boresight and center of phase positioning on ground

Antenna positions and boresight axis are measured on ground via combination of unit characterizations and satellite assembly metrology campaign via photogrammetry.

Photogrammetry is a 3-dimensional coordinate measuring technique that uses many two-dimensional photographs taken from different view angles. The fundamental principle used is triangulation in between target locations on several pictures. Processing is a combination of camera resection, target triangulation and bundle adjustment

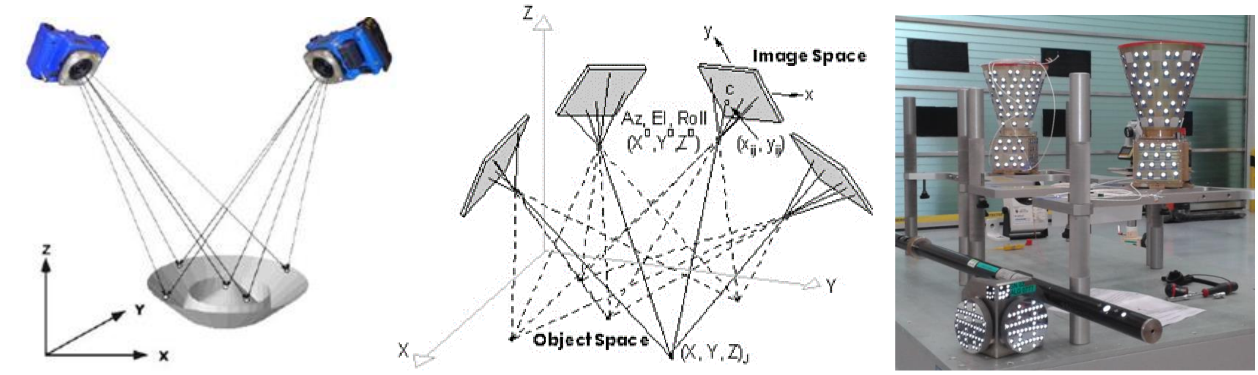

Figure 20 : Photogrammetry uses multiple photographs from different view point (left). Triangulation from all photographs is performed to retrieve object location (middle). Objects are equipped with dedicated targets (right)

On SWOT satellite, given the number of targets and the scales at play, and for antennas benefiting from a direct measurement, the typical residual error after ground measurement is 0.05 mm and 0.005 °.

As mentioned before, GPSP antenna does not feature any metrology device, and thus relies on strict machining tolerances to guarantee its position knowledge. Based on the detailed structural design, the positioning error is derived by accounting for machining tolerances, slack in joints and assembly imperfections. Given the absence of measurement, the positioning error is directly counted as position knowledge error.

5.2 Antennas boresight and center of phase displacement in flight

Thermoelastic distortion is the sole effect that impacts the antennas position and orientation with respect to the satellite reference frame. Moreover, we explained above that only satellite body and KaRIn arms distortion directly impact this knowledge.

Given the limited contribution, and the complexity of deriving and validating a temporal thermoelastic model representative of the satellite on its drifting orbit with extremely variable illumination, the thermoelastic distortion on satellite body and KaRIn masts are directly counted as errors in the overall budget.
This results in an uncertainty of less than 1 mm, compliant with margin with the allocated uncertainty.

GPSP flight displacement due to thermo-elastic	Axis	GPSP antenna TE displacement	Req. 2350	Margin wrt requirement
	Unit	[mm]	[mm]	[%]
Allocation	dx	0.10	1.5	x10
	dy	0.18		x5
	dz	0.99		52%

Figure 20 : Thermoelastic effects on GPSP antenna position relative to payload reference.

5.3 Satellite center of mass position

Satellite center of mass position is built from a model, gathering on-ground measurements results and inflight telemetry. Every one of the model assumptions, parameters or input data comes with its own uncertainty and error. We already detailed in chapter 4 the expected accuracy for predicting remaining propellant mass, propellant center of mass location and solar arrays center of mass. Here, we combined those uncertainties with all the other posts leading to satellite level center of mass location error estimations.

As described in §2.4, the accepted error on the center of mass position reconstruction is apportioned differently on different time scales :

- Bias : 6 mm per axis
- Long term errors : 4 mm per axis
- Orbital errors : 1.5 mm per axis

5.3.1 Static errors and uncertainties

Static errors are defined as all errors which will not vary after the end of the LEOP phase and before the re-entry phase beginning.
It includes Assembly Integration and Test measurement error on satellite mass and center of mass, covering both the measurement uncertainty, and the fact that the measured configuration was slightly different from the flight configuration. While differences have been compensated analytically, the operation still increases the error budget.
Static errors also include payload deployment uncertainties, 0g impact, and reference frame position characterization errors.
Finally, the propellant center of mass knowledge error, directly dependent on the tank diaphragm shape at launch, is a major share of the total error (see §4.1).

Combining all those effects leads to derivation of the potential error on center of mass position knowledge at satellite level. It reaches 3.2mm on the radial axis, which is still significantly better than the apportioned error tolerance of 6mm.

5.3.2 Orbital variations

SWOT science mission relies on satellite stability over long time-scales. As a consequence, no mission operations involve a satellite configuration change at orbital timescales. Consequently, orbital variations are limited to thermo-elastic effects. They are modelled at platform, payload and solar arrays levels, then subsystem center of mass displacement under thermal loads is computed and injected as errors in the satellite center of mass model.

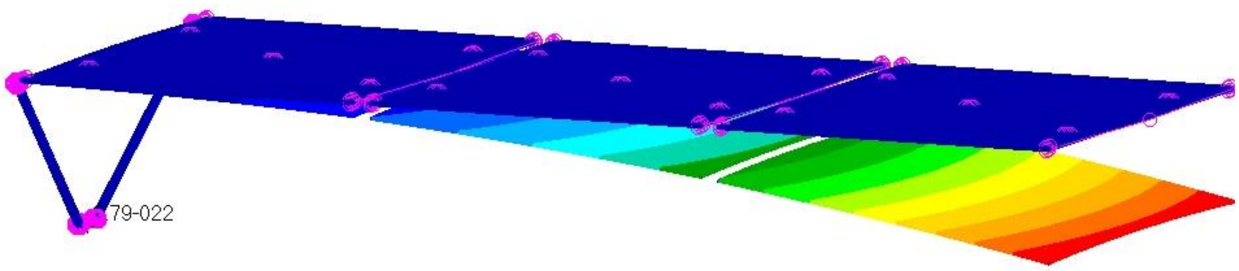

Figure 21 : Representation of the SWOT's solar array deformed when it's loaded by a thermal gradient across wing. To make the view comprehensible, the deformed wing doesn't respect the real scale.

Given potential correlation between the thermos-elastic effects worst cases (same illumination for all sub-systems), the platform, payload and solar arrays effects are combined linearly to derive the associated maximum error on center of mass position knowledge at satellite level. It reaches 0.55mm on the radial axis, which is still significantly better than the apportioned error tolerance of 1.5mm.

5.3.3 Long term drift

Long term part includes all errors posts potentially changing with time scales over 10 days. As a consequence, it covers post related to propellant mass after considering the modeling prediction. It also covers for residual solar arrays mass and deployed center of mass errors, as well as rotation axis characterization errors. A payload contribution linked to seasonal thermoelastic effect is accounted for.
After combination, the maximum error on center of mass position knowledge at satellite level is computed and reaches 3mm on the axial axis, compliant with allocation of 4mm.

5.3.4 Synthesis

Satellite center of mass position knowledge tolerated error has been split into 3 frequency ranges to better relate the SWOT mission needs with its dimensions. Indeed, meeting a Jason-like 5mm maximum error on SWOT satellite was deemed- unfeasible during the development. However, this performance being directly related to the height error, the best efforts have been deployed to minimize the residual uncertainties.
At the end, performances on all frequencies meet their allocation. In addition, linear sum of all those errors lead to total impact on POD performance on less than 6mm / axis. This is a significant achievement almost meeting the Jason-like requirements on this 2 tons and 5 m high satellite.

Error frequency ranges		Center of mass location Uncertainty @ Obs level [mm]		
		X	Y	Z
Total Static Error	bias	2.35	2.57	3.18
Long term error Budget	long term	3.06	3.09	2.23
Orbital Error Budget	orbital	0.33	0.36	0.55
Maximum POD error budget due to satellite center of mass position knowledge error	Total	5.7	6	6

Figure 22 : synthesis of satellite center of mass position uncertainties considering all frequency ranges.

6 FIRST FLIGHT FEEDBACK ON POD PERFORMANCES

SWOT satellite has been launched on December 16th. Since then, it went through commissioning, and calibration / validation period. After nine months in orbit, first flight correlations are available and show very promising results, both in the science data quality, and the POD performances.
Concerning POD validation and errors estimation, the accuracy of orbit determination can be assessed in flight by several metrics:

- the comparison between different orbit solutions
- the analysis of the residuals of high elevation SLR measurements.

These data are provided by different teams using different softwares and similar though not identical techniques (see [2] for more details).
An example of performance estimation is given Figure 22. This figures illustrated the independent orbit validation using SLR observations. Subset of highest quality ILRS stations already demonstrate radial POD accuracies lower than 1.2 cm (RMS).

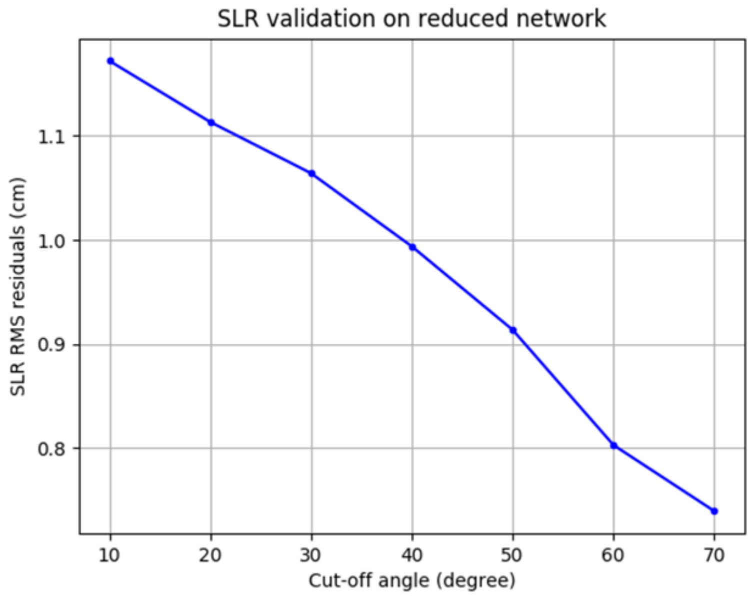

Figure 23– Estimation of Satellite Laser Ranging residuals versus elevation (against Doris+GPSP CNES orbit solution)

In addition, the presented analytical method to predict satellite center of mass had not needed any empirical corrections in flight. During checkout, only potential errors on the vector from the satellite reference to the DORIS or GPS phase center have been identified and tuned, as part of static components calibration.

The performance level is estimated better than 1.2 cm, based on the residual estimation of two independent orbit solutions, which is better than requirements. Moreover, no specific on-orbit perturbation is observed (for instance following SA rotations or after orbit control boost). This gives positive indication that the satellite modeling is correct, and that the satellite POD instrument vectors are well known after calibration, with no additional variations affecting the measurements.

7 CONCLUSION

This paper shows how the SWOT satellite development team has accounted for the challenges of the POD needs on a large and heavy spacecraft. It covered the derivation of requirement on specific bandwidth, reflecting the science needs without over constraining the satellite, and the individual contribution identification and quantification. Then it addressed the modelling approach defined to predict the satellite center of mass location, and discussed the remaining uncertainties which are well below the apportioned allocation. Finally, it presented early SWOT flight POD results.
In overall, the flight data confirms the good representativeness of the analytical approach, the performance compliance with the science requirements, with no need to inject any correction to the a-priori prediction model. It demonstrates that POD performance is aligned with the excellent first science performances of the SWOT mission.

8 REFERENCES

[1] Daniel Esteban Fernandez (JPL, USA) *SWOT Project. Mission Performance and error budget,* SWOT_D-79084, https://swot.jpl.nasa.gov

[2] Alexandre Couhert (CNES, France), Shailen Desai (JPL, USA), Sabine Houry (CNES, France), John Moyard (CNES, France), Flavien Mercier (CNES, France), *Early SWOT POD results*, OSTM 2023